Supplementary Material Available: A listing of hydrogen atom coordinates and the observed and calculated structure factor amplitudes is available (40 pages). Ordering information is given on any current masthead page.

References and Notes

(1) Author to whom correspondence should be sent at the Department of Chemistry, Florida State University, Tallahassee, Florida 32306.
(2) J. P. Collman, R. R. Gagne, T. R. Halbert, J. C. Marchon, and C. A. Reed, *J. Am. Chem. Soc.*, **96**, 2629 (1974); J. P. Collman, R. R. Gagne, C. A. Reed, and W. T. Robinson, *Proc. Natl. Acad. Sci. U.S.A.*, **71**, 1326 (1974); J. Almog, J. E. Baldwin, R. L. Dyer, and M. Peters, *J. Am. Chem. Soc.*, **97**, 226 (1975); J. E. Baldwin and J. Huff, *ibid.*, **95**, 5757 (1973).
(3) J. Geibel, C. K. Chang, and T. G. Traylor, *J. Am. Chem. Soc.*, **97**, 5926 (1975), and references cited therein.
(4) D. G. Pillsbury and D. H. Busch, unpublished results.
(5) S-M. Peng and V. L. Goedken, *J. Chem. Soc., Chem. Commun.*, 62 (1973); S-M. Peng and V. L. Goedken, *Inorg. Chem.*, in press. The formation of noncyclic tetradentate ligands from the metal template condensation reactions of hydrazones with carbonyls has also been recently reported (C. M. Kerwin and G. A. Melson, *ibid.*, **11**, 726 (1972)).
(6) F. G. Riddell and P. Murray-Rust, *Chem. Commun.*, 1075 (1970).
(7) M. Suh and V. L. Goedken, to be submitted for publication. The macrobicyclic nitrogen cage recently reported by Sargeson et al. (I. I. Creaser, J. MacB. Harrowfield, A. J. Herlt, A. M. Sargeson, J. Springborg, R. J. Geue, and M. R. Snow, *J. Am. Chem. Soc.*, **99**, 3182 (1977)) probably proceeds through a similar intermediate.
(8) "International Tables for X-Ray Crystallography", Vol. I, 2nd ed, Kynoch Press, Birmingham, England, pp 89 and 101.
(9) Reference 8, p 150.
(10) The obtainment of the refined lattice constants and the data collection was facilitated by the automatic diffractometer control program of Lenhert. P. G. Lenhert, *J. Appl. Crystallogr.*, **8**, 568 (1975).
(11) W. Busing and H. A. Levy, *J. Chem. Phys.*, **26**, 563 (1957); P. W. R. Corfield, R. Doedens, and J. A. Ibers, *Inorg. Chem.*, **6**, 197 (1967).
(12) Computations were performed on an IBM 370 computer with the aid of the following programs: Zalkin's FORDAP Fourier Program, Busing and Levy's ORFFF function and error program, and Iber's NUCLS least-squares program. Plots of the structures were drawn with the aid of C. K. Johnson's ORTEP.
(13) Neutral atom scattering factors were taken from D. T. Cromer and J. B. Mann, *Acta Crystallogr., Sect. A*, **24**, 321 (1968). Hydrogen atom scattering factors were taken from "International Tables for X-Ray Crystallography", Vol. III, Kynoch Press, Birmingham, England, 1962.
(14) D. T. Cromer, *Acta Crystallogr.*, **18**, 17 (1965).
(15) M. R. Churchill, *Inorg. Chem.*, **12**, 1213 (1973).
(16) E. L. Pace and L. J. Noe, *J. Chem. Phys.*, **49**, 5317 (1968).
(17) F. A. Cotton and F. Zingales, *J. Am. Chem. Soc.*, **83**, 351 (1961).
(18) P. Krumholz, *Struct. Bonding (Berlin)*, **9**, 129 (1971), and references cited therein.
(19) The number in parentheses following each distance denotes the mean of the estimated standard for the chemically equivalent bond distances.
(20) S. Brükner and L. Randaccio, *J. Chem. Soc. Dalton Trans.*, 1017 (1974), and references cited therein.
(21) M. D. Glick, W. G. Schmonsees, and J. F. Endicott, *J. Am. Chem. Soc.*, **96**, 5661 (1974).
(22) C. C. Costain, *J. Chem. Phys.*, **29**, 864 (1958); L. F. Thomas, E. I. Sherrard, and J. Sheridan, *Trans. Faraday Soc.*, **51**, 619 (1955).
(23) G. R. Clark, B. W. Skelton, and T. N. Waters, *J. Chem. Soc., Dalton Trans.*, 1528 (1976).
(24) M. C. Weiss, B. Bursten, S-M. Peng, and V. L. Goedken, *J. Am. Chem. Soc.*, **98**, 8021 (1976).
(25) M. J. D'Aniello, Jr., M. T. Mocella, F. Wagner, E. K. Barefield, and I. C. Paul, *J. Am. Chem. Soc.*, **97**, 194 (1975).
(26) M. D. Glick, J. M. Kuszaj, and J. F. Endicott, *J. Am. Chem. Soc.*, **95**, 5098 (1973).

Contribution No. 5649 from the Arthur Amos Noyes Laboratory of Chemical Physics, California Institute of Technology, Pasadena, California 91125, and Contribution from the IBM Research Laboratories, San Jose, California 95193

Further Studies of Metal–Metal Bonded Oligomers of Rhodium(I) Isocyanide Complexes. Crystal Structure Analysis of $[Rh_2(CNPh)_8](BPh_4)_2$

KENT R. MANN, NATHAN S. LEWIS, ROGER M. WILLIAMS, HARRY B. GRAY,* and J. G. GORDON II

Received August 15, 1977

The room-temperature electronic absorption spectra of $[Rh(CNR)_4]^+$ (R = Ph, *i*-Pr, cyclohexyl, *t*-Bu, vinyl) in solution do not follow Beer's law. This behavior has been attributed to oligomerization of $Rh(CNR)_4^+$ units to form species of the type $[Rh_n(CNR)_{4n}]^{n+}$. Band maxima attributable to oligomers are as follows: R = Ph, 568 nm (n = 2), 727 nm (n = 3), in acetonitrile solution; R = *t*-Bu, 490 nm (n = 2), 622 nm (n = 3), in aqueous solution; R = *i*-Pr, 495 nm (n = 2), 610 nm (n = 3), in aqueous solution; R = cyclohexyl, 516 nm (n = 2), in acetonitrile solution; R = vinyl, 555 nm (n = 2), 715 nm (n = 3), 962 nm (n = 4), in aqueous solution. The molar extinction coefficients (ϵ_n) and formation constants K_{n-1} have been obtained for R = Ph in acetonitrile solution and R = *t*-Bu in aqueous solution. Parameter values are as follows: for R = Ph, K_1 = 35 (15) M^{-1}, ϵ_2 = 1.05 (20) × 10^4, $\epsilon_3 K_2$ = 1.83 (40) × 10^5 M^{-1}; for R = *t*-Bu, K_1 = 250 (125) M^{-1}, ϵ_2 = 1.69 (34) × 10^4. The x-ray crystal structure of $Rh(CNPh)_4BPh_4$ has been completed (final R = 0.057). The compound crystallizes in the *Pbcn* space group (a = 23.80 (1), b = 19.23 (1), c = 19.08 (1) Å) with four discrete cationic $[Rh_2(CNPh)_8]^{2+}$ units and eight BPh_4^- anions. The dimeric cation has idealized D_{4d} symmetry; the two $[Rh(CNPh)_4]^+$ units are bonded face to face so as to give a staggered configuration of ligands. The Rh–Rh distance is 3.193 Å. The electronic absorption spectra of D_{4d} $[Rh_2(CNR)_8]^{2+}$ and assumed D_{4h} $[Rh_3(CNR)_{12}]^{3+}$ complexes are interpreted in terms of the interactions expected between the occupied $a_{1g}(d_{z^2})$ and unoccupied $a_{2u}[p_z, \pi^*(CNR)]$ monomer orbitals. The lowest band in each of the $[Rh_2(CNR)_8]^{2+}$ complexes is assigned to the allowed $1b_2 \rightarrow 2a_1$ transition. In the spectra of $[Rh_3(CNR)_{12}]^{3+}$ complexes, the lowest band is attributed to $2a_{1g} \rightarrow 2a_{2u}$.

We are continuing systematic investigations of the ground- and excited-state physical and chemical properties of complexes in which metal(d^8)–metal(d^8) interactions[1-4] are present. Systems that we have singled out for extensive study are based on planar rhodium(I) isocyanides.[4-7] In previous work we have established[4] that $[Rh(CNPh)_4]^+$ units oligomerize in acetonitrile solutions, yielding species such as $[Rh_2(CNPh)_8]^{2+}$ and $[Rh_3(CNPh)_{12}]^{3+}$. The dimeric and trimeric complexes are characterized by intense low-lying electronic absorption bands, which fall at 568 and 727 nm, respectively. These electronic spectral characteristics coupled with infrared spectral results led us to propose[4] that the structures of these oligomers feature face-to-face contact of $[Rh(CNPh)_4]^+$ units, with weak, direct Rh(I)–Rh(I) bonds. Purple crystalline samples of $Rh(CNPh)_4BPh_4$ have now been obtained, whose electronic spectra strongly suggest that dimeric $[Rh_2(CNPh)_8]^{2+}$ units are present. This paper reports the crystal structure analysis of $Rh(CNPh)_4BPh_4$, as well as additional detailed spectral studies of the oligomerization reactions of several $[Rh(CNR)_4]^+$ complexes in solution.

* To whom correspondence should be addressed at California Institute of Technology.

Experimental Section

The starting materials $[Rh(COD)X]_2$ (X^- = Cl^-, Br^-) were prepared by the method of Chatt and Venanzi.[8] Phenyl, isopropyl, cyclohexyl,

0020-1669/78/1317-0828$01.00/0 © 1978 American Chemical Society

and *tert*-butyl isocyanides were prepared via the Hoffman carbylamine reaction.[9] Vinyl isocyanide was prepared by the method of Matteson and Bailey.[10] Spectrograde solvents (CH_3CN, $CHCl_3$, C_6H_6) were used for recrystallization and spectral measurements. Elemental analyses were performed by Schwarzkopf Microanalytical Laboratory.

$Rh(CNR)_4X$ ($X^- = Cl^-$, BF_4^-, PF_6^-, BPh_4^-). These complexes were prepared by a standard method;[11] in each case an excess of the appropriate isocyanide was added slowly to a warm benzene solution of $[Rh(COD)Cl]_2$. A precipitate formed immediately and was filtered, washed with cold benzene and then ether, and air-dried.

Crude $Rh(CNR)_4Cl$ obtained above was dissolved in the minimum amount of water and filtered, and the solution was then added to a saturated aqueous solution of $NaBF_4$. The resulting precipitate was recrystallized from acetonitrile. Similar methods were used to synthesize BPh_4^- and PF_6^- salts using $NaBPh_4$ and KPF_6, respectively.

$Rh(CNPh)_4BF_4$. Anal. Calcd: C, 55.80; H, 3.30; N, 9.30; Rh, 17.10. Found: C, 55.67; H, 3.84; N, 9.32; Rh, 16.84. $\bar{\nu}$(CN) 2160 cm^{-1} (CH_2Cl_2 solution); brown crystals.

$Rh(CNPh)_4BPh_4$. Anal. Calcd: C, 74.85; H, 4.8; N, 6.72. Found: C, 74.59; H, 4.82; N, 6.76. $\bar{\nu}$(CN) 2160 cm^{-1} (CH_2Cl_2 solution); purple crystals.

$Rh(CNPh)_4PF_6$. Anal. Calcd: C, 50.92; H, 3.03; N, 8.49; Rh, 15.50. Found: C, 50.66; H, 3.22; N, 8.39; Rh, 14.58. $\bar{\nu}$(CN) 2160 cm^{-1} (CH_2Cl_2 solution); yellow crystals.

$Rh(CN\text{-}i\text{-}Pr)_4PF_6$. Anal. Calcd: C, 36.65; H, 5.38; N, 10.69. Found: C, 36.36; H, 5.22; N, 10.63. $\bar{\nu}$(CN) 2160 cm^{-1} (Nujol mull); violet crystals.

$Rh(CN\text{-}i\text{-}Pr)_4BPh_4$. Anal. Calcd: C, 68.79; H, 6.93; N, 8.01. Found: C, 68.51; H, 6.97; N, 7.97. $\bar{\nu}$(CN) 2160 cm^{-1} (Nujol mull); yellow crystals.

$Rh(CN\text{-}c\text{-}Hx)_4BF_4$. Anal. Calcd: C, 53.69; H, 7.08; N, 8.94. Found: C, 53.53; H, 7.00; N, 9.00. $\bar{\nu}$(CN) 2160 cm^{-1} (Nujol mull); purple crystals.

$Rh(CN\text{-}t\text{-}Bu)_4Cl$. Anal. Calcd: C, 51.01; H, 7.71; N, 11.90; Cl, 7.53. Found: C, 50.94; H, 7.85; N, 11.64; Cl, 7.36. $\bar{\nu}$(CN) 2160 cm^{-1} (CH_2Cl_2 solution); yellow crystals.

$Rh(CN(vinyl))_4Cl$. In a typical preparation, 2.0 g of $[Rh(COD)Cl]_2$ was placed in a side-arm flask on a vacuum line and about 5–10 mL of ether was distilled in from a solution of ether containing sodium benzophenone ketyl. An ampule containing approximately 3.5 g of vinyl isocyanide and about 3 g of ethanol was cooled in liquid N_2, broken, and quickly placed in a flask which was placed on the line. It was evacuated for about 1 or 2 min, and the contents were distilled into the reaction flask which was cooled with liquid nitrogen. After the contents were warmed to room temperature and stirred for about 20 min, the flask was taken off the line and the contents were filtered. The resultant powder was pumped dry overnight; yield 2.7 g, 95%. Anal. Calcd: C, 41.11; H, 3.46; N, 15.98; Rh, 29.35; Cl, 10.11. Found: C, 40.92; H, 3.45; N, 15.67; Rh, 29.12; Cl, 10.14. $\bar{\nu}$(CN) 2170 cm^{-1} (KBr pellet); black powder.

$Rh(CN(vinyl))_4X$ ($X^- = ClO_4^-$, BF_4^-). Perchlorate and tetrafluoroborate salts of tetrakis(vinyl isocyanide)rhodium(I) were prepared by reaction of about 5–10-fold excess of $NaClO_4$ or $NaBF_4$ with the chloride complex in acetonitrile. These complex salts were completely precipitated if an equal volume of water was added to the acetonitrile solution originally saturated with the chloride salt. Purification was effected by Soxhlet extraction of the solids with acetonitrile. Anal. Calcd: C, 34.76; H, 2.92; N, 13.51; Rh, 24.82; Cl, 8.55. Found: C, 34.22; H, 3.08; N, 13.12; Rh, 24.60; Cl, 8.80.

Spectral Data. Absorption spectra were measured using a Cary 17 spectrophotometer. Spectra were obtained in 1.00-, 0.1-, and 0.006-cm cells, all of which were calibrated with K_2CrO_4 solutions.[12] Infrared spectra were measured using a Perkin-Elmer 457 infrared spectrophotometer. The equilibrium constant determinations were based on absorption spectra obtained as a function of the concentration of $Rh(CNPh)_4PF_6$ in 0.1 M $(n\text{-}Bu_4N)PF_6$/acetonitrile at 25 (1) °C and $Rh(CN\text{-}t\text{-}Bu)_4Cl$ in 0.1 M NaCl/water at 25 (1) °C. Equilibrium was reached in all cases within the time of mixing. Data are available in Supplementary Tables 1 and 2.

X-Ray Data Collection. Long purple needles of $Rh(CNPh)_4BPh_4$ were obtained by slow evaporation of an acetonitrile solution. The crystals belong to the orthorhombic system with eight molecules in the unit cell. Cell parameters, obtained from a least-squares fit to the setting angles of 29 reflections using Ni-filtered Cu Kα radiation, are a = 23.80 (1), b = 19.23 (1), c = 19.08 (1) Å. The calculated density, 1.269 (1) g/cm^3, agrees well with 1.264 (3) g/cm^3 measured by flotation in CCl_4/heptane. Systematic absences uniquely identified the space group as *Pbcn*.

The crystals chosen for data collection resembled six-sided pillars bounded by the ⟨010⟩ and ⟨110⟩ faces with irregular ends (the 001 directions). These had been broken from longer (5–15 mm) needles and had approximate dimensions of 0.13 × 0.20 × 0.33 mm along a, b, and c, respectively. The needles were fragile and did not show clear cleavage planes perpendicular to the needle direction (c axis). The crystals were mounted with their c axes slightly misaligned with the ϕ axis of a Datex automated General Electric quarter-circle diffractometer. Intensity data were collected using Ni-filtered Cu Kα radiation and a θ–2 θ scan technique with a proportional counter. The takeoff angle was 3°. Reflections from the first crystal were measured at a scan speed of 1 °/min and backgrounds were counted for 20 s at each end of the scan. The scan width varied linearly with 2θ, having values of 1.8° at 2θ = 4° and 3.0° at 2θ = 130 °. The intensities of four check reflections, measured every 25 reflections, decreased with time, indicating significant radiation damage to the crystal, although there was no visible deterioration. As this crystal had already been exposed to the x-ray beam for a considerable time in the preliminary photographic investigation, a new crystal was mounted and data were collected in shells from 2θ = 4° to 2θ = 80° at a scan rate of 2°/min with 20-s background counts at the extremes of a scan. Data from the two crystals were corrected for background, Lorentz and polarization effects, and radiation decay, placed on a common scale, and merged, with the check reflections being averaged. The linear decay correction and the intercrystal scale factor were derived from the check reflection data. No correction for absorption was made (μ = 35.7 cm^{-1}).

Observational variances were computed from counting statistics with an empirical correction term $[(0.02S)^2$, where S is the scan count] to account for statistical errors.[13] We have found the factor 0.02 to be appropriate in this laboratory. After deletion of the systematic absences for *Pbcn* ($0kl$, k odd; $h0l$, l odd; $hk0$, $h + k$ odd), 2820 independent reflections were available.

Solution and Refinement of the Structure. An attempt to solve the structure by direct methods (MULTAN) failed, so standard heavy-atom methods were used. A three-dimensional Patterson synthesis revealed the positions of the rhodium atom and three of the coordinated C≡N groups. All remaining nonhydrogen atoms were found from a succession of Fourier synthesis and least-squares refinements. This was a tedious procedure because the rhodium atom lies very near x = 0 and, consequently, contributes significantly only to the $h + k$ even reflections.

All calculations were performed on an IBM 370/155 computer using the CRYM crystallographic computing system. Atomic scattering factors for C, N, and B were taken from ref 14, whereas the hydrogen factors are those of Stewart, Davidson, and Simpson for bonding hydrogen.[15] The rhodium scattering factors were those reported by Forsyth and Wells[16] for neutral rhodium and included anomalous dispersion. The quantity minimized in the least-squares calculations was $\sum w(F_o^2 - (1/s^2)F_c^2)^2$, where the weights are $w = 1/\sigma^2(F_o^2)$ and s is a scale factor. Full-matrix least-squares refinement was used with the scale factor and coordinates in one matrix and the temperature factors in another. Hydrogen parameters were not refined. The coordinates were calculated assuming a C–H distance of 0.96 Å. Temperature factors were fixed at $B_H = B_C + 1.5$ and were not changed after anisotropic temperature parameters were introduced for the carbon atoms. For the final least-squares cycles, anisotropic temperature parameters were assigned to all nonhydrogen atoms in the complex cation and isotropic temperature factors to all other atoms. The final R index ($R = \sum||F_o| - |F_c||/\sum F_o$) is 0.057 and the final "goodness-of-fit" $(\sum w(F_o^2 - F_c^2)/(m-s))^{1/2}$ is 2.63. On the last cycle, no parameter except the temperature factors associated with C11–C15 shifted by more than 0.5 of its standard deviation. Phenyl ring C11–C16 exhibited exceptionally large thermal motion throughout the refinement. The final calculated and observed structure factors are given in Supplementary Table 3. The calculated hydrogen atom positions are set out in Table I.

Solution Spectra

Absorption spectra for $Rh(CNR)_4X$ complexes at low concentration ($<10^{-4}$ M) show four bands whose positions are given in Table II. Slight changes in the band maxima occur on varying the R group when R = alkyl, but with R = vinyl or Ph the first two systems fall at distinctly lower energies.

Table I. Calculated Positions (×10⁴) and Isotropic Temperature Factors for Hydrogen Atoms

Atom	*x*	*y*	*z*	*B*, Å²
H6	−120	3357	1145	8.30
H7	−557	4333	671	8.70
H8	−1461	4267	225	9.80
H9	−1945	3223	292	11.60
H10	−1516	2247	751	9.70
H12	2014	847	982	15.10
H13	3045	1009	1222	18.10
H14	3142	1901	2042	13.90
H15	2556	2282	2864	17.10
H16	1585	1981	2632	13.60
H18	236	−1765	803	9.80
H19	373	−2972	901	10.80
H20	704	−3410	1956	9.36
H21	930	−2704	2878	9.66
H22	796	−1486	2763	8.88
H24	−1522	−615	2958	9.53
H25	−2413	−1081	3230	11.40
H26	−3145	−906	2449	9.83
H27	−3050	−184	1511	9.15
H28	−2173	307	1248	8.83
H30	385	3947	5	6.80
H31	−117	4433	−909	7.34
H32	320	4621	−1979	7.81
H33	1228	4274	−2144	8.84
H34	1751	3771	−1195	8.02
H36	2059	4578	−166	9.11
H37	3017	4915	44	10.50
H38	3631	4079	443	10.70
H39	3328	3041	854	10.40
H40	2379	2689	660	9.20
H42	608	2407	353	8.25
H43	496	1225	20	8.23
H44	1192	718	−672	9.59
H45	1955	1332	−1036	10.70
H46	2094	2490	−658	9.31
H48	1146	4630	749	7.50
H49	752	4931	1823	7.75
H50	582	4106	2657	7.37
H51	783	2958	2428	8.11
H52	1158	2627	1336	7.92

These low-concentration spectra resemble those of square-planar Rh(I) complexes containing phosphorus-donor ligands.[17]

New bands appear as the concentration of complex increases.[4] Representative absorption spectra for three different concentrations of $Rh(CNPh)_4PF_6$ in acetonitrile solution are shown in Figure 1. The bands at 361, 411, and 468 nm, which dominate the low-concentration spectra, decrease in intensity and two new bands grow in, first at 568 and then at 727 nm. The anion does not play a role in the spectral changes, as the BPh_4^- and BF_4^- salts exhibit identical behavior. These observations are best interpreted in terms of an oligomerization of the complex rhodium cations

$$2M \overset{K_1}{\rightleftharpoons} D$$

$$D + M \overset{K_2}{\rightleftharpoons} T$$

where M = $[Rh(CNPh)_4]^+$, D = $[Rh_2(CNPh)_8]^{2+}$, and T = $[Rh_3(CNPh)_{12}]^{3+}$. In our analysis of these equilibria we have utilized eq 1 and 2 where [Rh] is the total Rh concentration

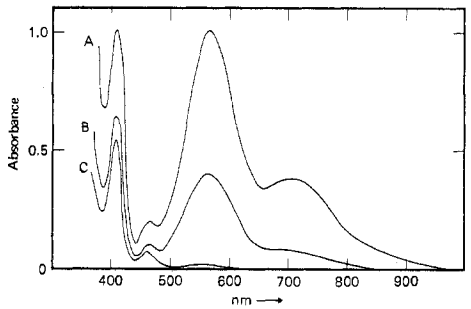

Figure 1. Absorption spectra of $Rh(CNPh)_4PF_6$ in acetonitrile solution at 25 °C: A, [Rh] = 5.7 × 10⁻² M, path length 0.06 mm; B, [Rh] = 2.7 × 10⁻² M, path length 0.06 mm; C, [Rh] = 6.3 × 10⁻⁴ M, path length 0.75 mm.

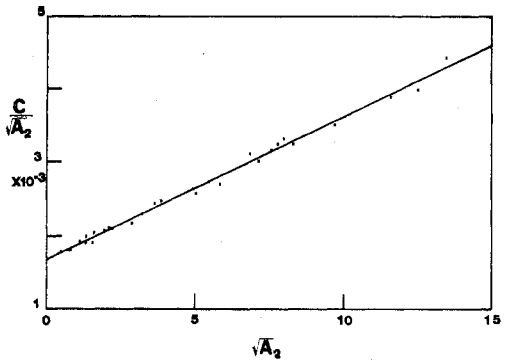

Figure 2. Plot of $[Rh]/A_2^{1/2}$ vs. $A_2^{1/2}$ for $Rh(CNPh)_4PF_6$ over the range 5 × 10⁻² M > [Rh] > 5 × 10⁻⁴ M in 0.01 M $(n\text{-}Bu_4N)PF_6$/CH_3CN solution; C ≡ [Rh].

$$\frac{[Rh]}{A_2^{1/2}} = \frac{1}{(\epsilon_2 K_1)^{1/2}} + \frac{2A_2^{1/2}}{\epsilon_2} + \frac{3K_2A_2}{\epsilon_2(\epsilon_2K_1)^{1/2}} \quad (1)$$

$$A_3 = (\epsilon_3 K_2 A_2^{3/2})/\epsilon_2(\epsilon_2K_1)^{1/2} \quad (2)$$

in terms of monomer, A_2 and A_3 are the absorbances due only to dimers and trimers, and ϵ_2 and ϵ_3 are the corresponding molar extinction coefficients.

A plot of $[Rh]/(A(568\text{ nm}))^{1/2}$ vs. $(A(568\text{ nm}))^{1/2}$ over the concentration range 5 × 10⁻² M > [Rh] > 5 × 10⁻⁴ M at constant ionic strength, 0.1 M $(n\text{-}Bu_4N)PF_6$, is a straight line (Figure 2), identifying the absorption peak at 568 nm as due to a dimer. The third term in eq 1 is unimportant, as there is no deviation from linearity even at higher concentrations. From the slope $(2/\epsilon_2)$ and intercept $(1/(\epsilon_2K_1)^{1/2})K_1 = 35$ (15) M^{-1} and $\epsilon_2 = 1.05$ (20) × 10⁴ are obtained. A plot of A_3 vs. $(A(568\text{ nm}))^{3/2}$ (eq 2) is also a straight line (Figure 3) with slope $\epsilon_3K_2/\epsilon_2(\epsilon_2K_1)^{1/2} = 2.92$ (60) × 10⁻². Substituting in the values of K_1 and ϵ_2 gives $\epsilon_3K_2 = 1.83$ (40) × 10⁵ M^{-1}. Estimating[18] ϵ_3 to be 1.8 × 10⁴ gives $K_2 = 10$ M^{-1}.

Table II. Absorption Spectral Data for $[Rh(CNR)_4]^+$ Complexes[a]

Complex		$^1A_{1g} \rightarrow {}^1E_u$	$^1A_{1g} \rightarrow {}^3E_u$	$^1A_{1g} \rightarrow {}^1A_{2u}$	$^1A_{1g} \rightarrow {}^3A_{2u}$
$Rh(CNEt)_4ClO_4$[b]		307 (24.4)	333 (3.45)	380 (8.40)	434 (0.26)
$Rh(CN\text{-}i\text{-}Pr)_4BPh_4$[c]		310 (28.0)	338 (3.80)	383 (11.2)	442 (0.34)
$Rh(CN\text{-}c\text{-}Hx)_4BF_4$[c]		310 (32.8)	338 (4.20)	383 (11.8)	442 (0.39)
$Rh(CN\text{-}t\text{-}Bu)_4Cl$[c]		310 (25.5)	335 (3.40)	386 (9.90)	442 (0.30)
$Rh(CN(vinyl))_4BF_4$[d]	233 (34.0)[e]	329 (19.0)	*f*	409 (5.0)	457 (0.7)
$Rh(CNPh)_4BPh_4$[g]	241 (60.5)[e]	335 (40.2)	*f*	411 (5.00)	463 (0.63)
$Rh(CNPh)_4PF_6$[g]	241 (59.2)[e]	335 (49.1)	*f*	411 (5.94)	462 (0.67)
$Rh(CNPh)_4BF_4$[g]	241 (59.4)[e]	335 (47.7)	*f*	411 (5.71)	463 (0.66)

[a] Band positions are given in nm; $\epsilon \times 10^{-3}$ values (±10%) are given in parentheses. [b] Taken from ref 27. [c] Determined at room temperature in CH_2Cl_2 solution. [d] Determined at room temperature in acetonitrile solution; band positions and intensities are virtually the same in the spectrum of the ClO_4^- salt. [e] Intraligand absorption. [f] Not observed. [g] Determined at room temperature in acetonitrile solution.

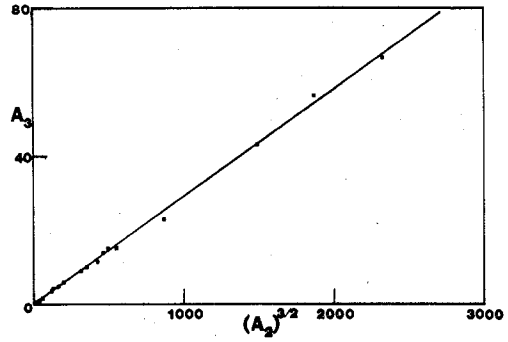

Figure 3. Plot of A_3 vs. $A_2^{3/2}$ for $Rh(CNPh)_4PF_6$ in 0.1 M (n-$Bu_4N)PF_6/CH_3CN$ solution.

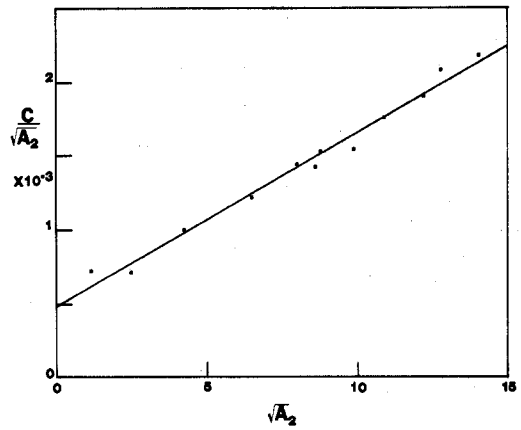

Figure 4. Plot of $[Rh]/A_2^{1/2}$ vs. $A_2^{1/2}$ for $Rh(CN\text{-}t\text{-}Bu)_4Cl$ over the concentration range 3×10^{-2} M > [Rh] > 1.6×10^{-4} M in 0.1 M $NaCl/H_2O$ solution; C ≡ [Rh].

Table III. Positions (nm) of the Lowest Intense Band in the Spectra of $[Rh_n(CNR)_{4n}]^{n+}$ Complexes

Complex	$n = 1$	$n = 2$	$n = 3$	Solvent
$Rh(CNPh)_4BPh_4$	411	568	727	CH_3CN
$Rh(CN\text{-}t\text{-}Bu)_4Cl$	371	490	622	H_2O
$Rh(CN\text{-}i\text{-}Pr)_4Cl$	383	495	610	H_2O
$Rh(CN\text{-}i\text{-}Pr)_4PF_6$	383	505	Not obsd	CH_3CN
$Rh(CN\text{-}c\text{-}Hx)_4BF_4$	383	516	Not obsd	CH_3CN
$Rh(CN(vinyl))_4BF_4$	403	555	715[a]	H_2O

[a] In concentrated solutions an additional band is observed at 962 nm; this band might be due to a tetrameric species.

The positions of the absorption bands attributable to oligomers of the various $[Rh(CNR)_4]^+$ complexes are set out in Table III. The vinyl and alkyl isocyanide complexes do not oligomerize appreciably in acetonitrile solution until concentrations very near the solubility limit are reached. They do oligomerize in aqueous solutions, as evidenced by analogous concentration-dependent absorption spectra. Only $Rh(CN\text{-}t\text{-}Bu)_4Cl$ was examined in detail in aqueous solution. The dimer of this complex absorbs at 490 nm. A plot of $[Rh]/A_2^{1/2}$ vs. $A_2^{1/2}$ for this band is again a straight line (Figure 4) whose slope and intercept yield $\epsilon_2 = 1.69\ (34) \times 10^4$ and $K_1 = 250\ (125)$ M^{-1}. An absorption at 622 nm, assigned to the trimer, is present only at very high concentrations, precluding a detailed analysis.

Crystal Structure of $Rh(CNPh)_4BPh_4$

Purple crystals of $Rh(CNPh)_4BPh_4$ contain discrete $[Rh_2(CNPh)_8]^{2+}$ cations and tetraphenylborate anions. The molecular structure of the cation is illustrated in Figures 5 and 6. Important bond angles and distances are given in Table IV. Refined coordinates and anisotropic thermal parameters for the cation and anion are set out in Tables V and VI, respectively.

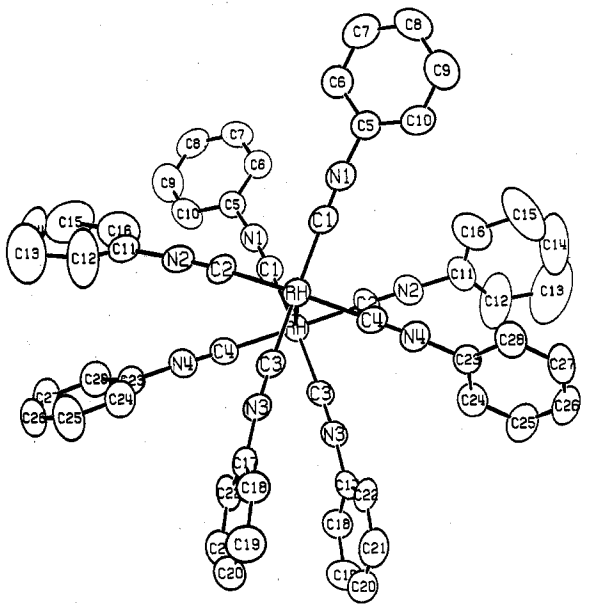

Figure 5. View of the molecular structure of the dimeric cation $[Rh_2(CNPh)_8]^{2+}$.

Table IV. Important Bond Distances (Å) and Angles (deg) in $[Rh_2(CNPh)_8]^{2+}$

	Distances		
Rh-Rh	3.193 (0)	C3-N3	1.146 (9)
Rh-C1	1.936 (7)	C4-N4	1.128 (9)
Rh-C2	1.957 (8)	C1-C5	1.396 (10)
Rh-C3	1.915 (7)	N2-C11	1.438 (11)
Rh-C4	1.972 (7)	N3-C17	1.404 (10)
C1-N1	1.164 (9)	N4-C23	1.417 (9)
C2-N2	1.134 (10)		
	Angles		
C1-Rh-C2	92.2 (3)	Rh-C2-N2	172.9 (7)
C2-Rh-C3	89.8 (3)	Rh-C3-N3	177.6 (6)
C3-Rh-C4	89.1 (3)	Rh-C4-N4	174.0 (7)
C4-Rh-C1	89.9 (3)	C1-N1-C5	174.5 (7)
C1-Rh-C3	169.6 (3)	C2-N2-C11	177.1 (8)
C2-Rh-C4	174.4 (3)	C3-N3-C17	175.0 (7)
Rh-C1-N1	173;0 (7)	C4-N4-C23	177.3 (7)

The cation has idealized D_{4d} symmetry and consists of two square-planar $[Rh(CNPh)_4]^+$ units connected to each other via a metal–metal bond, the ligands adopting a staggered configuration. The only crystallographically required symmetry is a C_2 axis perpendicular to the metal–metal bond. The Rh–Rh distance in the dimer is 3.193 Å, suggesting that the metal–metal bond in this complex is relatively weak. The Rh–Rh distance of 3.193 Å is considerably longer than that in Rh metal (2.69 Å)[19] or in Rh(0) and Rh(II) compounds where there is a conventional single bond. For example, the Rh–Rh distance in $[Rh(CO)(PPh_3)_2]_2$[20] is 2.630 Å and that in $Rh_2(DMG)_2(PPh_3)_2 \cdot H_2O \cdot C_3H_7OH$ is 2.936 Å.[21] The Rh–Rh distance in $[Rh_2(CNPh)_8]^{2+}$ is comparable to distances usually observed only in chloro-bridged d^8 complexes such as $[RhCl(CO)(PMe_2Ph)]_2$ (3.167 Å)[22] and $[Rh(CO)_2Cl]_2$ (3.12 Å).[23]

The RhC_4 coordination geometry is very nearly square planar, although deviations from the best least-squares plane through the $Rh(-C{\equiv}N)_4$ unit indicate a slight tetrahedral distortion. The average Rh–C–N and C–N–C angles are 174° and 176°, respectively. These are well within the normal range for coordinated isocyanides (compare 176° observed for both angles in $[RhI(fumaronitrile)P(OC_6H_5)_3(p\text{-}CH_3OC_6H_4NC)_2]$[24] and 174° and 176°, respectively, in $cis\text{-}PtCl_2(CNEt)(PEt_2Ph)$[25]). The average metal–carbon bond length, 1.94 Å, is comparable to the 1.96 Å reported for $[RhI(fumaronitrile)P(OC_6H_5)_3(p\text{-}CH_3OC_6H_4NC)_2]$[24] but longer than

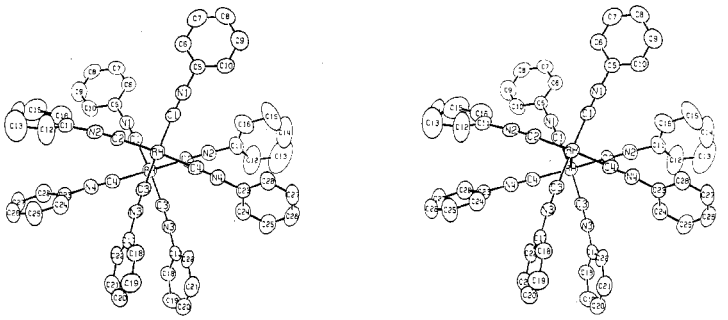

Figure 6. Stereoview of $[Rh_2(CNPh)_8]^{2+}$ looking down the C_2 axis that bisects the Rh–Rh bond.

Table V. Refined Coordinates and Anisotropic Thermal Parameters for the Cation[a,b]

Atom	x	y	z	U_{11}	U_{22}	U_{33}	U_{12}	U_{13}	U_{23}
Rh	−409 (2)	6 927 (3)	16 650 (4)	651 (4)	702 (4)	878 (5)	−57 (4)	−1 (5)	49 (4)
C1	−3 330 (29)	16 080 (39)	14 511 (43)	731 (53)	670 (57)	807 (71)	−93 (45)	125 (54)	58 (61)
N1	−5 211 (23)	21 318 (34)	12 545 (34)	746 (47)	743 (50)	793 (58)	−66 (40)	33 (46)	50 (54)
C5	−7 844 (32)	27 222 (41)	9 830 (43)	723 (60)	706 (61)	741 (72)	−16 (52)	12 (61)	41 (63)
C6	−4 970 (32)	33 249 (45)	9 661 (47)	831 (64)	846 (69)	906 (78)	−9 (53)	8 (61)	32 (71)
C7	−7 551 (40)	38 959 (45)	6 863 (51)	1196 (79)	822 (68)	981 (89)	−185 (65)	229 (77)	−123 (71)
C8	−12 878 (42)	38 545 (47)	4 290 (59)	1200 (83)	853 (70)	1451 (108)	363 (65)	137 (87)	157 (85)
C9	−15 669 (38)	32 517 (61)	4 625 (64)	1019 (78)	1426 (100)	1722 (121)	69 (73)	−321 (86)	344 (105)
C10	−13 188 (37)	26 798 (43)	7 328 (54)	998 (71)	837 (67)	1379 (103)	−181 (59)	−294 (76)	286 (71)
C2	7 356 (31)	10 262 (37)	16 483 (50)	669 (56)	781 (56)	1149 (83)	−212 (48)	−141 (69)	174 (67)
N2	11 903 (27)	11 930 (29)	17 072 (37)	845 (48)	726 (44)	1003 (61)	−99 (42)	−109 (59)	257 (50)
C11	17 690 (35)	13 814 (43)	18 120 (55)	781 (71)	878 (71)	1225 (102)	−170 (59)	−237 (79)	423 (73)
C12	21 419 (49)	11 175 (79)	13 744 (75)	993 (94)	3293 (187)	1835 (144)	223 (111)	472 (104)	151 (142)
C13	27 449 (67)	12 242 (104)	14 640 (110)	1727 (154)	3954 (259)	3749 (278)	674 (157)	1205 (174)	1278 (242)
C14	27 662 (45)	17 164 (79)	20 071 (99)	733 (94)	2789 (186)	3711 (263)	−289 (91)	342 (119)	1446 (196)
C15	24 325 (60)	19 905 (69)	24 873 (83)	1824 (138)	2169 (137)	2709 (193)	−878 (134)	−1440 (163)	864 (154)
C16	18 825 (46)	18 057 (53)	23 425 (69)	1482 (96)	1259 (96)	1837 (145)	−202 (77)	−773 (105)	1 (96)
C3	2 254 (26)	−2 462 (35)	17 003 (43)	679 (50)	606 (52)	813 (67)	−101 (40)	−4 (53)	−39 (60)
N3	3 670 (22)	−8 160 (29)	17 131 (39)	651 (40)	574 (43)	1149 (64)	−89 (36)	70 (36)	8 (58)
C17	4 973 (28)	−15 268 (41)	17 610 (55)	463 (52)	764 (66)	1248 (94)	−100 (51)	−101 (66)	−92 (79)
C18	3 793 (33)	−19 573 (45)	12 308 (58)	834 (64)	741 (68)	1620 (111)	−43 (56)	−150 (75)	−11 (80)
C19	4 531 (39)	−26 642 (50)	12 865 (68)	1204 (86)	895 (75)	1893 (138)	−90 (70)	−270 (93)	−308 (93)
C20	6 561 (35)	−29 199 (46)	19 064 (79)	785 (68)	902 (76)	2385 (178)	72 (59)	−133 (96)	55 (101)
C21	7 862 (34)	−25 061 (53)	24 497 (64)	737 (64)	1196 (83)	1611 (114)	119 (66)	−140 (77)	287 (102)
C22	7 065 (28)	−17 913 (43)	23 810 (60)	474 (54)	993 (67)	1514 (107)	127 (51)	23 (67)	−115 (86)
C4	−8 147 (31)	3 437 (35)	17 811 (45)	753 (57)	627 (50)	919 (76)	−38 (46)	72 (66)	67 (58)
N4	−12 495 (24)	1 476 (29)	19 084 (35)	733 (45)	766 (48)	801 (59)	−69 (40)	3 (52)	−31 (46)
C23	−17 840 (29)	−1 258 (37)	20 839 (47)	632 (52)	717 (66)	738 (71)	11 (48)	−47 (64)	16 (60)
C24	−18 393 (33)	−5 274 (44)	26 592 (48)	804 (61)	1137 (80)	988 (95)	42 (56)	−80 (67)	254 (71)
C25	−23 564 (40)	−8 085 (50)	28 139 (58)	920 (71)	1620 (98)	1389 (106)	−234 (74)	129 (81)	610 (85)
C26	−27 904 (35)	−6 908 (47)	23 649 (66)	659 (60)	1317 (89)	1662 (131)	−199 (61)	249 (75)	8 (95)
C27	−27 305 (32)	−2 775 (49)	18 067 (59)	589 (55)	1409 (94)	1410 (111)	58 (55)	−218 (76)	71 (82)
C28	−22 217 (33)	135 (46)	16 500 (46)	819 (59)	1187 (72)	837 (77)	54 (63)	−180 (64)	88 (73)

[a] Coordinates have been multipled by 10^5 and thermal parameters by 10^4. [b] The complete temperature factor expression is $\exp[-2\pi^2(U_{11}h^2a^{*2} + U_{22}k^2b^{*2} + U_{33}l^2c^{*2} + 2U_{12}hka^*b^* + 2U_{13}hla^*c^* + 2U_{23}klb^*c^*)]$.

those observed in *cis*-$PtCl_2(CNPh)_2$ (1.90 Å)[25] and *cis*-$PtCl_2(CNEt)(PEt_2Ph)$ (1.83 Å).[26] The average bond lengths within the ligand are 1.14 (2) Å for C≡N and 1.41 (2) Å for N–C(phenyl). The dimensions of the phenyl rings are normal except for the one attached to C11, which shows unusually large thermal motion.

The tetraphenylborate anion is completely unexceptional. There are no short intermolecular contacts. The entire structure has relatively large thermal parameters, which may be attributable to the poor packing of the "flattened" $[Rh_2(CNPh)_8]^{2+}$ cations with the bulky BPh_4^- anions. The closest interdimer Rh–Rh distance is 6.893 (1) Å. All other interdimer Rh–Rh distances are at least one-half a unit cell edge. Thus it is clear that interdimer Rh–Rh electronic interactions may be neglected.

Electronic Structure and Spectral Assignments

An orbital energy order $b_{2g}(xy) < e_g(xz, yz) < a_{1g}(z^2) \ll a_{2u} < b_{1g}(x^2 - y^2)$ is expected for monomeric $[Rh(CNR)_4]^+$ complexes.[27] The energy of the lowest spin-allowed band (assigned as the $^1A_{1g} \rightarrow {}^1A_{2u}$ ($a_{1g} \rightarrow a_{2u}$) transition) increases in the order phenyl (411 nm) ~ vinyl (409 nm) < isopropyl (383 nm) (Table II). This accords with the expected stabilization of the a_{2u} orbital via conjugation with the π system

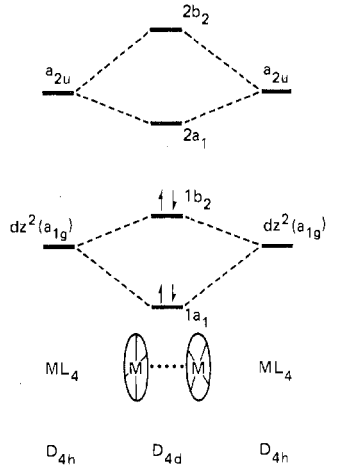

Figure 7. Relative energies of the molecular orbitals derived from $a_{1g}(d_{z^2})$ and a_{2u} monomer functions in D_{4d} $[Rh_2(CNPh)_8]^{2+}$.

Table VI. Refined Coordinates and Isotropic Thermal Coordinates for the Tetraphenylborate Anion[a]

Atom	x	y	z	B, Å²
B1	1449 (3)	3385 (4)	128 (5)	4.78 (0.21)
C29	1112 (3)	3793 (3)	−487 (4)	4.57 (0.17)
C30	571 (3)	4006 (4)	−436 (4)	5.50 (0.18)
C31	267 (3)	4303 (4)	−977 (5)	5.93 (0.19)
C32	522 (3)	4405 (4)	−1602 (5)	6.74 (0.20)
C33	1052 (4)	4210 (4)	−1696 (5)	7.46 (0.22)
C34	1366 (3)	3902 (4)	−1127 (5)	6.41 (0.20)
C35	2121 (3)	3604 (4)	203 (4)	5.67 (0.19)
C36	2315 (3)	4248 (4)	36 (5)	7.73 (0.22)
C37	2889 (4)	4454 (5)	149 (6)	9.44 (0.27)
C38	3238 (4)	3970 (5)	410 (6)	9.01 (0.26)
C39	3069 (4)	3350 (5)	625 (6)	9.23 (0.26)
C40	2501 (4)	3142 (4)	518 (5)	7.62 (0.22)
C41	1368 (3)	2570 (4)	−72 (5)	5.66 (0.19)
C42	901 (3)	2187 (4)	86 (5)	6.76 (0.20)
C43	822 (3)	1484 (5)	−120 (5)	7.76 (0.23)
C44	1231 (4)	1194 (5)	−528 (5)	8.30 (0.24)
C45	1684 (4)	1548 (5)	−734 (6)	9.60 (0.27)
C46	1764 (3)	2240 (5)	−510 (5)	7.80 (0.23)
C47	1180 (3)	3580 (4)	899 (4)	4.27 (0.17)
C48	1065 (3)	4269 (4)	1082 (5)	5.90 (0.19)
C49	838 (3)	4453 (4)	1727 (5)	5.85 (0.19)
C50	737 (3)	3974 (4)	2212 (4)	5.91 (0.20)
C51	852 (3)	3305 (4)	2077 (5)	6.84 (0.21)
C52	1076 (3)	3108 (4)	1420 (5)	6.34 (0.20)

[a] Coordinates are given × 10⁴.

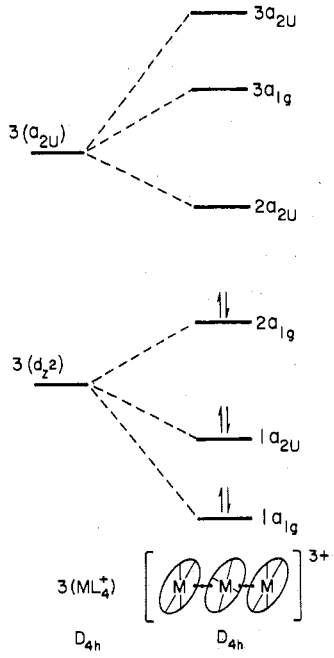

Figure 8. Relative energies of the molecular orbitals derived from $a_{1g}(d_{z^2})$ and a_{2u} monomer functions in D_{4h} $[Rh_3(CNR)_{12}]^{3+}$.

of the vinyl or phenyl group.[28] Other assignments accord with the detailed interpretation of the spectrum of $[Rh(CNEt)_4]^+$ given previously by Isci and Mason.[27]

In Table III are the positions of the lowest intense bands in the electronic spectra of the rhodium(I) isocyanide monomers and oligomers. The electronic spectral properties of a D_{4d} $[Rh_2(CNR)_8]^{2+}$ may be understood in terms of the orbital interactions diagrammed in Figure 7. The monomer orbitals that will interact most strongly in the dimers are those that extend perpendicular to the molecular plane, namely, the $a_{1g}(d_{z^2})$ and $a_{2u}[p_z, \pi^*(CNR)]$ functions. The $a_{1g}(d_{z^2})$- and a_{2u}-derived levels are comprised of orbitals of the same symmetry, and as a result there will be considerable mixing, stabilizing the lower set ($1a_1$, $1b_2$) and destabilizing the upper one ($2a_1$, $2b_2$). Because the lower set is filled, this stabilization is an important source of intermonomer binding.

Two allowed electronic transitions are predicted for the dimer, one higher ($1a_1 \rightarrow 2b_2$) and one lower ($1b_2 \rightarrow 2a_1$) than the $a_{1g} \rightarrow a_{2u}$ excitation in the monomer. Thus the bands at 563 nm in $[Rh_2(CNPh)_8]^{2+}$, 550 nm in $[Rh_2(CN(vinyl))_8]^{2+}$, and 490 nm in $[Rh_2(CN\text{-}t\text{-}Bu)_8]^{2+}$ are assigned to $1b_2 \rightarrow 2a_1$.

We have assumed a D_{4h} (staggered) rotameric configuration for the $[Rh_3(CNR)_{12}]^{3+}$ complexes in constructing the MO level diagram shown in Figure 8. The ground-state electronic configuration is $1a_{1g}{}^2 1a_{2u}{}^2 2a_{1g}$. Stabilization of the filled $1a_{1g}$ and $1a_{2u}$ levels may occur by mixing with unfilled orbitals of the same symmetry, as postulated for the dimers. Thus some degree of Rh–Rh–Rh bonding results. Five allowed electronic transitions are predicted involving the a_{1g} and a_{2u} trimer orbitals ($2a_{1g} \rightarrow 2a_{2u}$, $2a_{1g} \rightarrow 3a_{2u}$, $1a_{2u} \rightarrow 3a_{1g}$, $1a_{1g} \rightarrow 2a_{2u}$, $1a_{1g} \rightarrow 3a_{2u}$), the lowest of which ($2a_{1g} \rightarrow 2a_{2u}$) is assigned to the 727-nm band in $[Rh_3(CNPh)_{12}]^{3+}$. Bands attributable to $2a_{1g} \rightarrow 2a_{2u}$ transitions in trimeric species are also observed at 715 nm in $[Rh_3(CN(vinyl))_{12}]^{3+}$ and at 622 nm in $[Rh_3(CN\text{-}t\text{-}Bu)_{12}]^{3+}$.

Acknowledgment. We thank R. E. Marsh for helpful comments. Research at the California Institute of Technology was supported by the National Science Foundation (Grant No. CHE75-19086). Acknowledgment is also made to the donors of the Petroleum Research Fund, administered by the American Chemical Society, for partial support of this research. K.R.M. acknowledges a National Science Foundation Energy Postdoctoral Fellowship (1976–1977). Matthey-Bishop, Inc. is acknowledged for a generous loan of rhodium trichloride.

Registry No. $Rh(CNPh)_4BPh_4$, 65405-08-5; $Rh(CN\text{-}t\text{-}Bu)_4Cl$, 51139-75-4; $Rh(CN\text{-}i\text{-}Pr)_4Cl$, 65405-07-4; $Rh(CN\text{-}i\text{-}Pr)_4PF_6$, 51139-64-1; $Rh(CN\text{-}c\text{-}Hx)_4BF_4$, 65405-06-3; $Rh(CN(vinyl))_4BF_4$, 65405-05-2; $Rh(CNPh)_4BF_4$, 65405-04-1; $Rh(CNPh)_4PF_6$, 56192-49-5; $Rh(CN\text{-}i\text{-}Pr)_4BPh_4$, 65405-03-0; $Rh(CN(vinyl))_4Cl$, 65405-02-9; $Rh(CN(vinyl))_4ClO_4$, 65405-01-8; $Rh_2(CNPh)_8(BPh_4)_2$, 65405-18-7; $Rh_2(CN\text{-}t\text{-}Bu)_8Cl_2$, 65405-16-5; $Rh_2(CN\text{-}i\text{-}Pr)_8Cl_2$, 65405-15-4; $Rh_2(CN\text{-}i\text{-}Pr)_8(PF_6)_2$, 65405-14-3; $Rh_2(CN\text{-}c\text{-}Hx)_8(BF_4)_2$, 65405-12-1; $Rh_2(CN(vinyl))_8(BF_4)_2$, 65405-10-9; $Rh_3(CNPh)_{12}(BPh_4)_3$, 65405-26-7; $Rh_3(CN\text{-}t\text{-}Bu)_{12}Cl_3$, 65405-24-5; $Rh_3(CN\text{-}i\text{-}Pr)_{12}Cl_3$, 65405-23-4; $Rh_3(CN(vinyl))_{12}(BF_4)_3$, 65405-22-3; $Rh_4(CN(vinyl))_{16}(BF_4)_4$, 65405-20-1; $[Rh(COD)Cl]_2$, 12092-47-6.

Supplementary Material Available: Absorption spectral data for $Rh(CNPh)_4PF_6$ in 0.1 M $(n\text{-}Bu_4N)PF_6/CH_3CN$ and for $Rh(CN\text{-}t\text{-}Bu)_4Cl$ in 0.1 M $NaCl/H_2O$ and observed and calculated structure factors (18 pages). Ordering information is given on any current masthead page.

References and Notes

(1) J. S. Miller and A. J. Epstein, *Prog. Inorg. Chem.*, **20**, 1 (1976).
(2) D. S. Martin, Jr., R. M. Rush, R. F. Kroening, and P. E. Fanwick, *Inorg. Chem.*, **12**, 301 (1973).
(3) H. Isci and W. R. Mason, *Inorg. Chem.*, **13**, 1175 (1974).
(4) K. R. Mann, J. G. Gordon II, and H. B. Gray, *J. Am. Chem. Soc.*, **97**, 3553 (1975).
(5) N.S. Lewis, K. R. Mann, J. G. Gordon II, and H. B. Gray, *J. Am. Chem. Soc.*, **98**, 7461 (1976).
(6) V. M. Miskowski, G. L. Nobinger, D. S. Kliger, G. S. Hammond, N. S. Lewis, K. R. Mann, and H. B. Gray, *J. Am. Chem. Soc.*, **100**, 485 (1978).
(7) K. R. Mann, N. S. Lewis, V. M. Miskowski, D. K. Erwin, G. S. Hammond, and H. B. Gray, *J. Am. Chem. Soc.*, **99**, 5525 (1977).
(8) J. Chatt and L. M. Venanzi, *J. Chem. Soc. A*, 4735 (1957).
(9) W. P. Weber, G. W. Gokel, and I. K. Ugi, *Angew. Chem., Int. Ed. Engl.*, **11**, 530 (1972).
(10) D. S. Matteson, and R. A. Bailey, *J. Am. Chem. Soc.*, **90**, 3761 (1968).
(11) J. W. Dart, M. K. Lloyd, R. Mason, and J. A. McCleverty, *J. Chem. Soc., Dalton Trans.*, 2039, 2046 (1973).
(12) G. W. Haupt, *J. Opt. Soc. Am.*, **42**, 441 (1952).
(13) W. R. Busing and H. A. Levy, *J. Chem. Phys.*, **26**, 563 (1957).
(14) "International Tables for X-Ray Crystallography", Vol. III, Kynoch Press, Birmingham, England, 1962, p 202.

(15) R. F. Stewart, E. R. Davidson, and W. T. Simpson, *J. Chem. Phys.*, **42**, 3175 (1965).
(16) J. B. Forsyth and M. Wells, *Acta Crystallogr.*, **12**, 412 (1959).
(17) G. L. Geoffroy, M. S. Wrighton, G. S. Hammond, and H. B. Gray, *J. Am. Chem. Soc.*, **96**, 3105 (1974).
(18) We have found[4,5] in several cases that $\epsilon_D \simeq 2\epsilon_M$. Therefore, we have made the reasonable assumption that $\epsilon_T \simeq 3\epsilon_M$.
(19) J. Donohue, "The Structures of the Elements", Wiley, New York, N.Y., 1974, p 216.
(20) P. Singh, C. B. Dammann, and D. J. Hodgson, *Inorg. Chem.*, **12**, 1335 (1973).
(21) K. G. Caulton and F. A. Cotton, *J. Am. Chem. Soc.*, **93**, 1914 (1971).
(22) J. J. Bonnet, Y. Jeannin, P. Kalck, A. Maisonnat, and R. Poilblanc, *Inorg. Chem.*, **14**, 743 (1975).
(23) L. F. Dahl, C. Martell, and D. J. Wampler, *J. Am. Chem. Soc.*, **83**, 1761 (1961).
(24) A. P. Gaughan, Jr., and J. A. Ibers, *Inorg. Chem.*, **14**, 3073 (1975).
(25) B. Jovanovic, Lj. Manojlovic-Muir, and K. W. Muir, *J. Chem. Soc., Dalton Trans.*, 1178 (1972).
(26) B. Jovanovic and Lj. Manojlovic-Muir, *J. Chem. Soc., Dalton Trans.*, 1176 (1972).
(27) H. Isci and W. R. Mason, *Inorg. Chem.*, **14**, 913 (1975).
(28) K. R. Mann, M. Cimolino, G. L. Geoffroy, G. S. Hammond, A. A. Orio, G. Albertin, and H. B. Gray, *Inorg. Chim. Acta*, **16**, 97 (1976).

Contribution from the Chemistry Division,
Argonne National Laboratory, Argonne, Illinois 60439

Structural Studies of Precursor and Partially Oxidized Conducting Complexes. 13. A Neutron Diffraction and X-Ray Diffuse Scattering Study of the Dimerized Platinum Chain in Rubidium Tetracyanoplatinate Chloride (2:1:0.3) Trihydrate, $Rb_2[Pt(CN)_4]Cl_{0.3}\cdot 3.0H_2O$[1]

JACK M. WILLIAMS,* PAUL L. JOHNSON, ARTHUR J. SCHULTZ, and CHRISTOPHER C. COFFEY[2]

Received August 17, 1977

The crystal structure and molecular formula of the one-dimensional conductor $Rb_2[Pt(CN)_4]Cl_{0.30}\cdot 3.0H_2O$, RbCP(Cl), have been fully characterized using single-crystal neutron diffraction, x-ray diffuse scattering data, and thermogravimetric analysis. We have determined that RbCP(Cl) is isostructural with KCP(Cl) and KCP(Br) except that only one halide site can be identified; i.e., there does not appear to be any evidence for the presence of a "defect" water molecule in RbCP(Cl). From thermogravimetric analyses RbCP(Cl) is a 3.0 hydrate as is KCP(Br). RbCP(Cl) crystallizes in the tetragonal space group *P4mm*, with unit cell dimensions $a = 10.142$ (6) Å, $c = 5.801$ (4) Å, $V_c = 596.7$ Å^3, and $Z = 2$. A total of 1113 neutron diffraction data (594 independent) were collected to $(\sin\theta)/\lambda = 0.724$ and of these 511 had $F_o^2 > \sigma(F_o^2)$. The crystal structure was solved using MULTAN and a full-matrix least-squares refinement resulted in a final $R(F_o^2) = 0.063$ (all data) and $R(F_o^2) = 0.059$ for data with $F_o^2 > \sigma(F_o^2)$. Using x-ray diffuse scattering techniques we have established the Pt oxidation as +2.31 (2) from which the molecular formula $Rb_2[Pt(CN)_4]Cl_{0.31(2)}\cdot 3.0H_2O$ is obtained. The structure consists of nearly planar $Pt(CN)_4$ moieties stacked along the *c* axis forming a perfectly linear Pt–Pt chain. The crystal asymmetric unit contains two independent $Pt(CN)_4^{1.7-}$ groups, two H_2O sites, one Rb^+ site, and one Cl^- site. The asymmetric ordering of the Rb^+ ion and the H_2O molecules constitutes the main source of crystal asymmetry. The two-independent Pt–Pt chain distances are definitely *unequal* (2.877 (8) and 2.924 (8) Å) with the average intrachain separation (2.90 Å) being slightly longer than in KCP(Br) (2.88 Å) and KCP(Cl) (2.87 Å). Since RbCP(Cl) and KCP(Cl) are isostructural, it appears that the replacement of K^+ by Rb^+ results in lattice expansion along *c*, which produces larger Pt–Pt intrachain separations, simply because of the larger cation radius of Rb^+. Thus the unequal and slightly longer Pt–Pt separations in RbCP(Cl), compared to those in KCP(Br, Cl), apparently result in increased electron localization along the Pt-atom chain and a concomitant decrease in the electrical conductivity.

Introduction

Partially oxidized tetracyanoplatinate (POTCP) compounds have currently been of great interest due in part to Little's predictions[3] of high-temperature superconductivity in one-dimensional metals. The room temperature metallic conductivities of these POTCP salts are due to the formation of Pt–Pt chains along which electron transport occurs. Usually these POTCP salts have metal–metal spacings only ~0.02–0.2 Å longer than in Pt metal (2.78 Å). Experience has shown that the electrical transport properties of these salts depend not only on the specific compound under study but also on the crystalline environment of the metal conducting spine.[24] For example, the chemical environment about the $Pt^{(2+x)+}(CN)_4$ ($x = 0.25$–0.40) groups results in *bent* metal chains in $K_{1.75}[Pt^{2.25+}(CN)_4]\cdot 1.5H_2O$ (Pt–Pt = 2.96 Å)[4] and *linear* chains in $K_2[Pt^{2.33+}(CN)_4]Br_{0.3}\cdot 3.0H_2O$ (Pt–Pt = 2.88 Å).[5] It has been shown[6,7] that the degree of partial oxidation (DPO) and the Pt–Pt spacings are inversely related, such that it is possible to predict one if the other is known. In the two known cases with the highest DPO's[8] (~0.40), in $Cs_2[Pt^{2.39+}(CN)_4](FHF)_{0.39}$ and $Rb_2[Pt^{2.40+}(CN)_4](FHF)_{0.40}$, the Pt–Pt spacings are the shortest yet observed[9] in POTCP salts at 2.83 and 2.80 Å, respectively. Because metal–metal bonds between Pt atoms are reported[10] to be as short as ~2.5–2.6 Å, it is not unreasonable to assume that Pt–Pt spacings in POTCP salts may eventually be found which will be considerably *less* than in Pt metal (~2.78 Å) itself.

In this paper we discuss the detailed molecular structure of $Rb_2[Pt(CN)_4]Cl_{0.3}\cdot 3.0H_2O$, RbCP(Cl), derived from a single-crystal neutron diffraction analysis. This study was undertaken to provide structural information which might assist in explaining why RbCP(Cl), which appears to be isostructural with KCP(Cl), has a maximum conductivity of ~0.1 that of KCP(Cl).[11] We also present new synthetic results which indicate that while RbCP(Cl) can be prepared, its Br^- analogue has yet to be synthesized. Therefore, as we previously postulated,[20] the report[23] of an x-ray diffuse scattering study of $Rb_2[Pt(CN)_4]Br_{0.25}\cdot 1.3H_2O$, RbCP(Br), may have actually been performed on $Rb_{1.75}[Pt(CN)_4]\cdot xH_2O$.

Experimental Section

Crystal Preparation. Attempts to prepare RbCP(Br) in the conventional manner by mixing $Rb_2[Pt^{4+}(CN)_4Br_2]$ and $Rb_2[Pt^{2+}(CN)_4]\cdot xH_2O$ in a 1:5 ratio, or in any ratio, at 5[25] or 22 °C were not successful, even if excess RbBr was present (vide infra). Furthermore, we were unable to synthesize it by electrolysis (2 V dc) of a solution of RbBr and $Rb_2[Pt(CN)_4]\cdot xH_2O$. However, we were able to prepare RbCP(Cl) by either of the above mentioned methods. Chemical analysis[12] yielded a composition consistent with $Rb_2[Pt(CN)_4]Cl_{0.3}\cdot 3H_2O$, and iodine–thiosulfate titrations[13] established the metal oxidation state as $Pt^{2.30+}$. Emission spectrographic analyses revealed that only Pt and Rb were present with traces of K (~0.08%)

0020-1669/78/1317-0834$01.00/0 © 1978 American Chemical Society